Photochemical Upconversion Approach to Broad-Band Visible Light Generation

Tanya N. Singh-Rachford, Radiy R. Islangulov, and Felix N. Castellano*

Department of Chemistry and Center for Photochemical Sciences, Bowling Green State University, Bowling Green, Ohio 43403

Received: December 30, 2007; In Final Form: January 28, 2008

The sensitized triplet−triplet annihilation (TTA) of 9,10-dimethylanthracene (DMA) upon selective excitation of $[Ru(dmb)_3]^{2+}$ (dmb = 4,4′-dimethyl-2,2′-bipyridine) at 514.5 nm in dimethylformamide (DMF) resulted in upconverted and downconverted DMA excimer photoluminescence. The triplet excited state of $[Ru(dmb)_3]^{2+}$ is efficiently quenched by 11 mM DMA in DMF resulting in photon upconversion but no excimer formation. The bimolecular quenching constant of the dynamic quenching process is 1.4×10^9 M^{-1} s^{-1}. At 90 mM DMA, both upconversion and downconversion processes are readily observed in aerated DMF solutions. The TTA process was confirmed by the quadratic dependence of the upconverted and downconverted emission emanating from the entire integrated photoluminescence profile (400−800 nm) of DMA measured with respect to incident light power. Time-resolved emission spectra of $[Ru(dmb)_3]^{2+}$ and 90 mM DMA in both aerated and deaerated DMF clearly illustrates the time-delayed nature of both types of singlet-state emission, which interestingly shows similar decay kinetics on the order of 14 μs. The emission quantum yields (Φ) measured using relative actinometry increased with increasing DMA concentrations, reaching a plateau at 3.0 mM DMA (Φ = 4.0%), while at 90 mM DMA, the overall quantum yield diminished to 0.5%. The dominant process occurring at 3.0 mM DMA is upconversion from the singlet excited state of DMA, whereas at 90 mM DMA, both upconversion and excimeric emission are observed in almost equal portions, thereby resulting in an overall broad-band visible light-emission profile.

Introduction

Remarkable progress has been afforded in the design and fabrication of advanced light-emitting device architectures.[1−3] Given current global energy concerns, a large effort has been expended on materials that produce white-light emission in the pursuit of highly efficient lighting, thereby minimizing electrical energy waste in daily applications.[4] Over the past few years, our group and others have shown that it is indeed possible to efficiently drive photon upconversion using low-power incoherent light sources and simple metal−organic molecular assemblies using sensitized triplet−triplet annihilation (TTA) photochemistry.[5,6] We recently translated these processes to the solid state[5e] and even utilized them to run uphill photochemical reactions.[5] In 2006, we made an observation that inspired the current study. When $Ir(ppy)_3$ (ppy is 2-phenylpyridine) was selectively excited in the presence of high concentrations of pyrene, we simultaneously detected upconverted singlet fluorescence and strong downconverted excimer emission emanating from pyrene.[5c] The latter process was derived from the sensitized TTA reaction and provided strong evidence that molecules susceptible to excimer formation may be exploited in new advanced materials that produce both upconverted and downconverted emissions with respect to monochromatic incident photons. Given that many organic light-emitting devices (OLEDs) and electroluminescence (EL) materials utilize annihilation processes for light generation, it is plausible that such a technology would be adaptable in these applications and may result in devices with low drive voltages.

The current paper describes a molecular assembly composed of a Ru(II) metal-to-ligand charge transfer (MLCT) sensitizer $[Ru(dmb)_3]^{2+}$ (dmb is 4,4′-dimethyl-2,2′-bipyridine) and 9,10-dimethylanthracene (DMA), an aromatic hydrocarbon known to produce low-energy excimer emission out to ~700 nm.[7] With 514.5 nm laser excitation at low flux, selective excitation of $[Ru(dmb)_3]^{2+}$ sensitizes ^{3}DMA*, which undergoes TTA, producing photon emission that spans almost the entire visible spectrum, 425−700 nm, with an emission color that is systematically variable with excitation power. All experiments described herein were performed in both air-saturated in addition to argon degassed solutions, the former being important from a

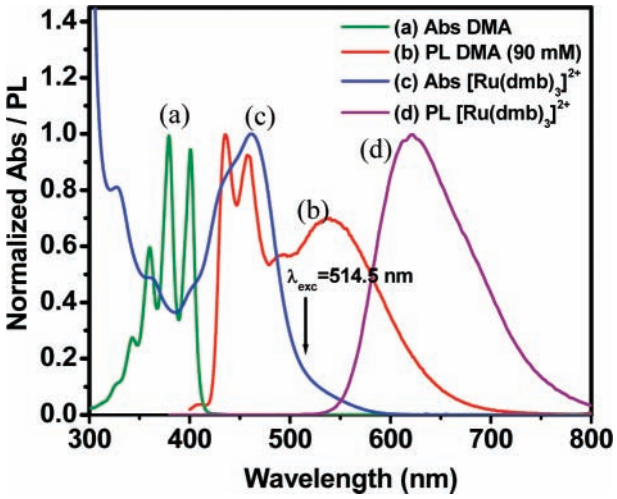

Figure 1. Normalized absorbance and photoluminescence of 90 mM DMA and optically dilute $[Ru(dmb)_3]^{2+}$ in DMF. The excitation wavelength used in this study to generate both upconverted and downconverted emissions is indicated: 514.5 nm.

* To whom correspondence should be addressed. Tel.: (419) 372-7513; fax: (419) 372-9809; e-mail: castell@bgsu.edu.

10.1021/jp712165h CCC: $40.75
Published on Web 03/21/2008

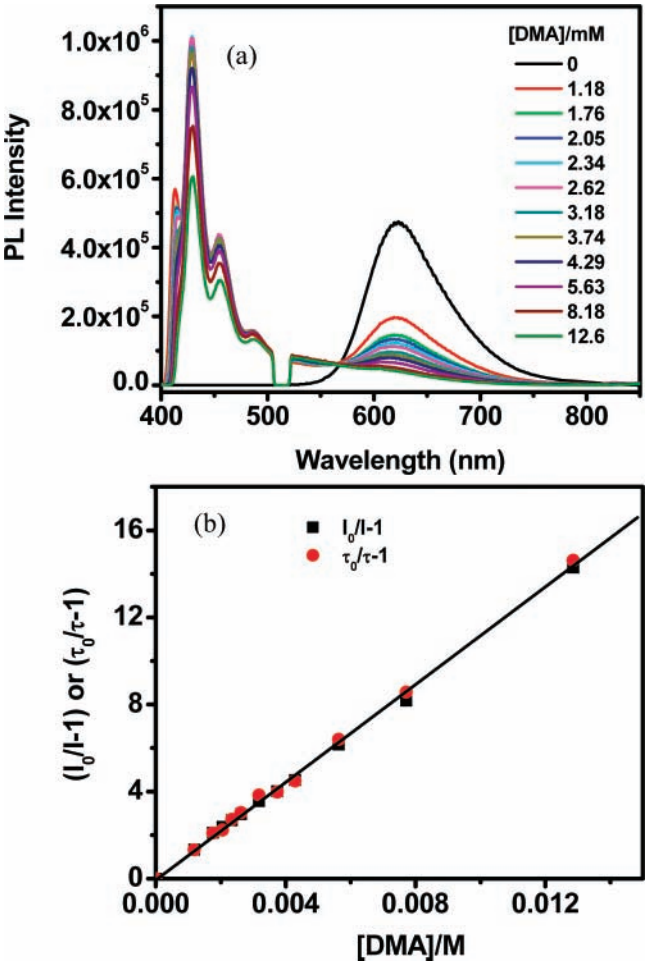

Figure 2. (a) Emission intensity plot of $[Ru(dmb)_3]^{2+}$ measured as a function of DMA concentration in deaerated DMF. (b) Stern−Volmer plot generated from both intensity and excited-state lifetime quenching of $[Ru(dmb)_3]^{2+}$ with DMA in deaerated DMF.

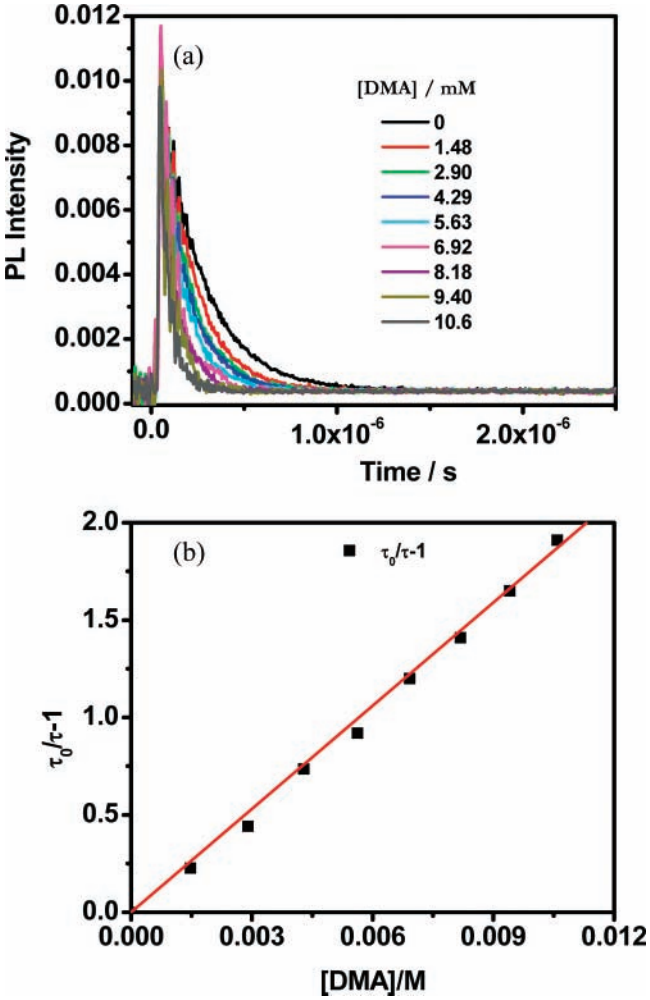

Figure 3. (a) Luminescence decay of $[Ru(dmb)_3]^{2+}$ measured as a function of DMA concentration in aerated DMF. (b) Stern−Volmer plot generated from the lifetime measurements of the quenching of $[Ru(dmb)_3]^{2+}$ with DMA in aerated DMF.

technological standpoint. Even under aerated conditions, the triplet-state processes governing the relevant light-producing reactions proceeded surprising well and are particularly noteworthy for potential real-world device applications.

Experimental Procedures

General. $Ru(dmb)_3(PF_6)_2$ was prepared according to the published procedure.[5] DMA (Aldrich), spectroscopic grade acetonitrile, and *N*,*N*-dimethylformamide (DMF) (Fisher Chemicals) were used as received.

Spectroscopic Measurements. The static absorption spectra were measured on a HP 8453 diode array spectrometer. Steady-state photoluminescence spectra were obtained with a single-photon counting spectrofluorimeter from Edinburgh Analytical Instruments (FL/FS 900). Excitation was accomplished using an argon ion laser (Coherent Innova 300) whose multi-line output was split using a diffraction grating, and the desired wavelength component of 514.5 nm was selected and passed through a narrow bandpass filter prior to incidence on the sample. A 514.5 ± 8 nm notch filter (Semrock) was placed in the emission path between the sample and the monochromator to remove scattered laser light from the emission profile. The excitation power density was measured using an Ophir Nova II optical power meter equipped with a photodiode detector head (PD300-UV). All samples were contained in 1 cm^2 anaerobic quartz cells from Starna Cells. Relative emission quantum yields were referenced to $[Ru(dmb)_3](PF_6)_2$ in CH_3CN ($\Phi = 0.073 \pm 0.006$),[8] using previously described procedures.[9] The complete spectral profile that combined both upconverted and downconverted integrated emission signals was used for relative quantum yield determinations in $[Ru(dmb)_3]^{2+}$/DMA mixtures. Even though the emission profile of the standard sample did not overlap the broad-band photoluminescence at short wavelengths, the experimentally determined quantum yields were very reproducible using the relative actinometry. Single-wavelength emission intensity decays were acquired with a N_2 pumped dye laser (2−3 nm fwhm) from PTI (GL-3300 N_2 laser, GL-301 dye laser) using an apparatus that was previously described.[9] Coumarin 510 was used to tune the unfocused pulsed excitation beam. Pulse energies were typically ~60 μJ/pulse, measured by placing a Molectron Joulemeter (J4−-05) at the sample position.

Time-resolved emission spectra were acquired in DMF solutions, using a computer controlled Nd:YAG laser Quantel/OPO system from OPOTEK (Vibrant-LD). A Micro HR Horiba/JY spectrograph equipped with a 300 gr/mm grating interfaced with an Andor iSTAR iCCD camera served as the detection system. The iCCD camera was synchronized with a DG535 digital delay generator (Stanford Research Systems) which was triggered from the laser flashlamp output. Typical experiments employed a gate width of 2 μs averaged over 100 laser shots. All data were collected from the Andor software and processed separately in Origin 7.5.

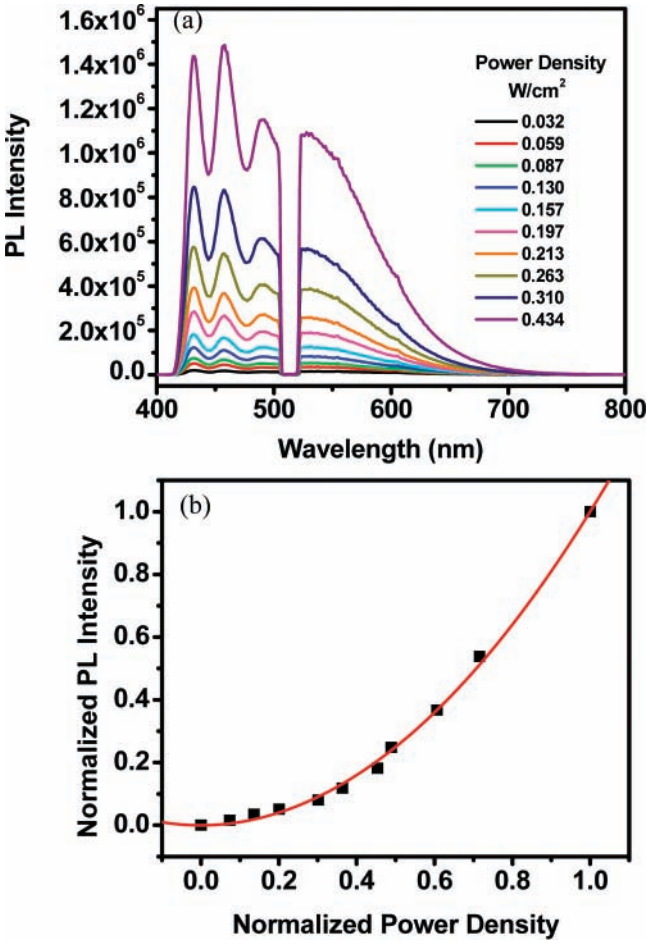

Figure 4. (a) Photoluminescence intensity profile of air-saturated DMF solutions of $[Ru(dmb)_3]^{2+}$ (3.6×10^{-5} M) + DMA (90 mM) as a function of 514.5 nm laser power density with a 514.5 nm notch filter in the emission path. (b) Normalized integrated emission intensity data from panel a plotted as a function of the normalized incident power density of the laser. The solid red line is the best quadratic fit to the integrated emission data, $x^{2.0}$.

Results and Discussion

Figure 1 presents the absorption and emission properties of both $[Ru(dmb)_3]^{2+}$ and 90 mM DMA in DMF solution; all emission spectra were measured using typical excitation conditions (Xe lamp/monochromator source) into each respective low-energy ground-state absorption band. The triplet charge-transfer emission of $[Ru(dmb)_3]^{2+}$ peaked at 622 nm, exhibiting lifetimes of 807 ± 2 and 190 ± 5 ns in argon deaerated DMF and aerated DMF, respectively. The red spectrum in Figure 1 illustrates that 90 mM DMA yields singlet fluorescence in the blue region in addition to strong excimeric emission at longer wavelengths between 500 and 700 nm.[7] The singlet and triplet energies of DMA previously were reported as ~25 000 and 14 700 cm^{-1},[10,11] respectively, thereby making DMA an attractive energy transfer quencher for the triplet excited state of $[Ru(dmb)_3]^{2+}$. The singlet fluorescence quantum yield of DMA in DMF was reported to approach unity in DMF, whereas the triplet quantum yield and lifetime of this chromophore in deaerated DMF were reported to be 0.02 and 4 ms, respectively.[7a]

The MLCT-based triplet emission of $[Ru(dmb)_3]^{2+}$ was efficiently quenched by energy transfer to DMA. Quantitative measurements of this quenching were determined by Stern−Volmer analysis from both photoluminescence intensity and excited-state lifetime quenching of $[Ru(dmb)_3]^{2+}$ with DMA in deaerated DMF (Figure 2). The Stern−Volmer relation is given in eq 1

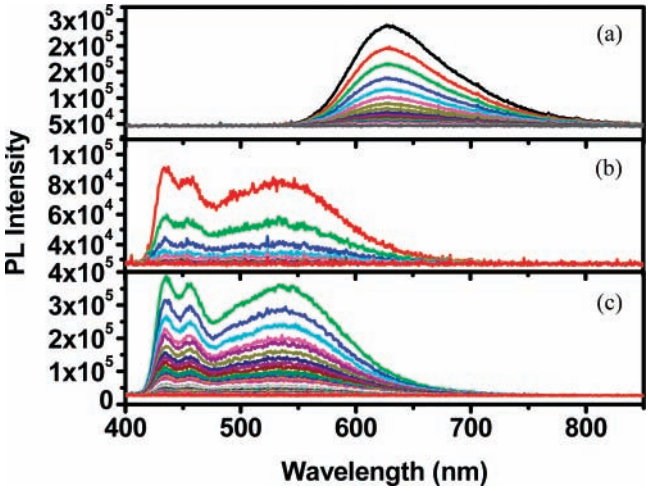

Figure 5. Time-resolved emission spectra of (a) 3.6×10^{-5} M $[Ru(dmb)_3]^{2+}$; (b) 3.6×10^{-5} M $[Ru(dmb)_3]^{2+}$ + 90 mM DMA (aerated); and (c) 3.6×10^{-5} M $[Ru(dmb)_3]^{2+}$ + 90 mM DMA in deaerated DMF upon 515 nm excitation at 5 mJ/pulse. Spectra were collected at 2 μs intervals.

$$I_0/I = \tau_0/\tau = 1 + K_{sv}[Q] \quad (1)$$

where I_0 and I represent the photoluminescence intensities in the absence and presence of the quencher, respectively, and τ_0 and τ are the lifetimes in the absence and presence of the quencher, respectively. K_{sv} is the Stern−Volmer constant, and [Q] is the molar concentration of the DMA energy transfer acceptor. K_{sv} is the product of k_q (bimolecular quenching constant in M^{-1} s^{-1}) and τ_0 (in s) is determined from both static and dynamic quenching experiments as 1101.5 M^{-1}, yielding $k_q = 1.4 \times 10^9$ M^{-1} s^{-1}, close to the diffusion limit in DMF[12,13] and consistent with the dynamic nature of the bimolecular energy transfer process. This is in reasonable agreement with the k_q value of 2.2×10^9 M^{-1} s^{-1} determined for the related energy transfer quenching process of $[Ru(bpy)_3]^{2+}$ (bpy = 2,2′-bipyridine) by anthracene in a 15:1 benzene/ethanol solution at 25 °C.[14] In the present work, quantitative quenching of the triplet excited state of $[Ru(dmb)_3]^{2+}$ was observed at approximately 13 mM DMA in deaerated DMF, which is also consistent with the previously reported quenching of $[Ru(bpy)_3]^{2+}$ by anthracene, where complete quenching was realized at a 15 mM quencher concentration.[14] While 13 mM DMA is sufficient to observe sensitized upconversion following selective excitation of $[Ru(dmb)_3]^{2+}$, many experiments in this study were performed at 90 mM DMA since at this concentration, almost equal portions of upconverted and downconverted photons resulted in the generation of white light.

The quenching of the triplet excited state of $[Ru(dmb)_3]^{2+}$ by DMA was also investigated in aerated DMF, where competitive quenching of $[Ru(dmb)_3]^{2+}$ occurred by both DMA and dissolved oxygen. Analysis of the triplet lifetime quenching of the sensitizer as a function of increasing DMA concentration in aerated DMF resulted in a linear plot, with a K_{sv} value of 197.4 M^{-1}, thereby resulting in a calculated k_q value of 1.04×10^9 M^{-1} s^{-1} ($\tau_0 = 190$ ns) (Figure 3). The triplet excited state of $[Ru(dmb)_3]^{2+}$ was completely quenched upon the addition of 10.6 mM DMA in aerated DMF. This lower value as compared to the deaerated solution (13 mM) accounts for the dissolved oxygen present in solution, which serves as a competitive ^{3}MLCT-state quencher. As similar bimolecular

SCHEME 1: Qualitative Energy Level Diagram of Upconversion Process Related to $[Ru(dmb)_3]^{2+}$ and DMA Resulting in Delayed Singlet DMA Fluorescence and Downconverted DMA Excimer Photoluminescence[a]

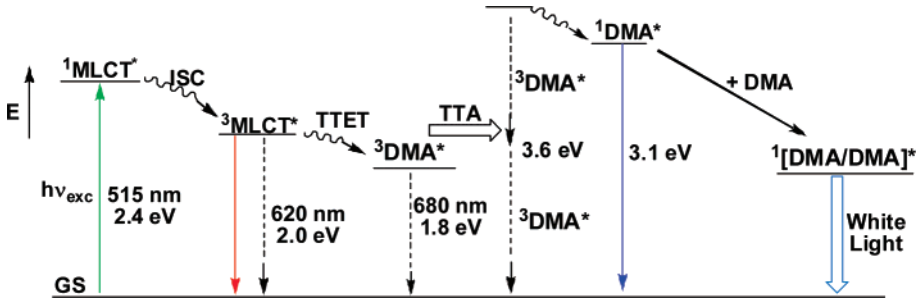

[a] Solid colored lines represent radiative processes. ISC is intersystem crossing, TTET is triplet−triplet energy transfer, and TTA is triplet−triplet annihilation.

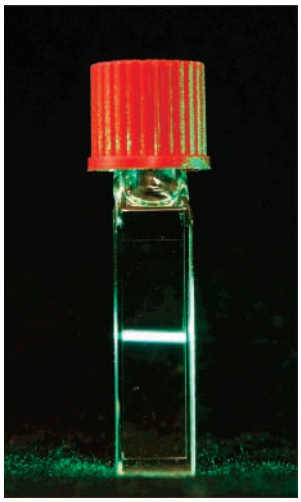

Figure 6. Digital photograph of the cell containing an air-saturated DMF solution of $[Ru(dmb)_3]^{2+}$ (3.6×10^{-5} M) + DMA (90 mM). Experimental conditions: $\lambda_{ex} = 514.5$ nm (Ar^+ laser) at 8 mW (0.13 W/cm^2).

quenching constants were observed in both aerated and deaerated DMF, we conclude that DMA is an effective triplet excited-state quencher of $[Ru(dmb)_3]^{2+}$, even in air-saturated solutions.

When a mixture of the two chromophores, $[Ru(dmb)_3]^{2+}$ (3.6×10^{-5} M) and DMA (90 mM), in aerated DMF was excited at 514.5 nm, the excitation intensity dependent emission spectra displayed in Figure 4a were produced. Careful inspection of the photoluminescence profile shown in Figure 4a shows a very small peak at about 610 nm, which is due to a Raman band from DMF. A notch filter, 514.5 ± 8 nm, was used to selectively exclude scattered laser light from the emission profile. As the incident power density was increased, the upconverted and downconverted emissions emanating from DMA increased in a quadratic fashion, illustrating that both processes are initiated by two sequential one-photon absorption processes.[5,6] Figure 4b displays the integrated emission intensity data from each spectrum in Figure 4a plotted as a function of normalized 514.5 nm incident power density. The red line in Figure 4b represents the best quadratic fit to the data set, $y = x^{2.0}$. The results indicate that the delayed fluorescence intensity is indeed proportional to the square of the incident power and hence to the square of the triplet concentration. To the best of our knowledge, this is the first quantitative example of a light power quadratic dependence that can be simultaneously applied to both upconversion and downconversion emanating from the same sample.

The time-resolved emission spectra of 3.6×10^{-5} M $[Ru(dmb)_3]^{2+}$ are displayed in Figure 5a, and this result was compared to the time-resolved emission spectra of 3.6×10^{-5} M $[Ru(dmb)_3]^{2+}$ and 90 mM DMA (aerated) (Figure 5b) in addition to the complementary experiment performed in argon degassed DMF (Figure 5c). The solutions were excited with 514.5 ± 3 nm laser pulses using a Nd:YAG/OPO system and gated-iCCD detection. From the time-resolved emission profile of both 3.6×10^{-5} M $[Ru(dmb)_3]^{2+}$ and 90 mM DMA in aerated and degassed solutions, the peak corresponding to the phosphorescence of the sensitizer in the power dependence study was not observed. It should be noted that similar concentrations of both the sensitizer and the acceptor were used in both studies. The quenching experiments that were discussed earlier also demonstrated that the triplet emission of $[Ru(bpy)_3]^{2+}$ was effectively quenched when 13.0 and 10.6 mM DMA in deaerated and aerated DMF were added to the sensitizer. These time-resolved emission spectra following selective pulsed laser excitation of $[Ru(dmb)_3]^{2+}$ also demonstrate the delayed nature of both types of singlet-state emission from DMA. Delayed fluorescence is a hallmark of the bimolecular TTA process,[5] and the production and decay of both emission types clearly occur on similar time scales. The time constant of the upconversion and excimer emission was determined in both aerated and deaerated solutions and is on the order of ~ 13 μs in both cases. Scheme 1 is the qualitative energy level diagram that illustrates the process of photon upconversion and downconversion in this system. Upon selective excitation of $[Ru(dmb)_3]^{2+}$, TTA of DMA occurs, resulting in the generation of a singlet excited DMA. Once the excited singlet state is produced, it decays by two distinct pathways that have similar efficiency and lifetimes and, hence, yield a broad-band emission that is well-balanced in color. This occurs, at least in part, as a result of working in aerated solutions where O_2 serves as a quencher of the triplet-state processes leading to both upconversion and downconversion.

The broad-band emission from these solutions is readily visualized and is white in visual appearance when inspected with the naked eye. Figure 6 displays a digital photograph of the light emission generated from the mixture of $[Ru(dmb)_3]^{2+}$ and 90 mM DMA in an aerated DMF solution during 514.5 nm excitation. The white-light emission is real and not an experimental artifact of CCD camera saturation. In fact, the relative emission quantum yields across the entire profile are quite variable, sharply increasing with increasing DMA concentration (Figure 7), which plateaus at 4.0% efficiency with 3.0 mM DMA; this emission corresponds primarily to upconversion fluorescence from the singlet state of DMA and does not contain any significant excimer contributions. Once the DMA concentration is raised to 90 mM, the relative quantum yield is diminished to 0.5% but now appears white in color as a result of containing almost equal portions of upconverted and

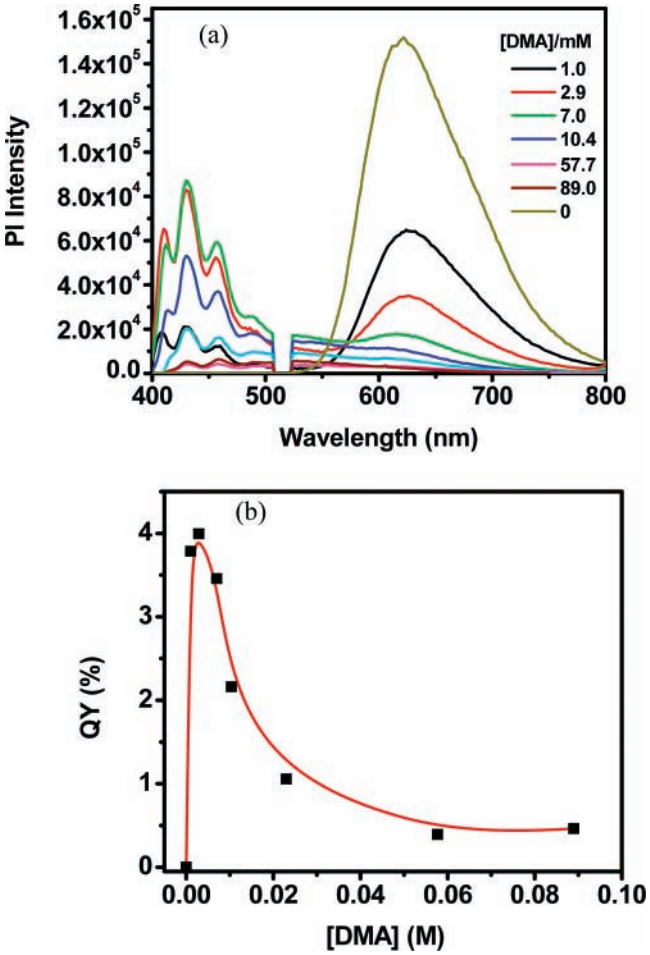

Figure 7. (a) Total emission profile of 3.6×10^{-5} M $[Ru(dmb)_3]^{2+}$ as a function of DMA concentration in aerated DMF. Experimental conditions: $\lambda_{ex} = 514.5$ nm (Ar^+ laser) at 8 mW incident power (0.13 W/cm^2), 514.5 nm notch filter in the emission path. (b) Quantum yield of upconversion measured relative to the $[Ru(dmb)_3]^{2+}$ standard as a function of increasing DMA concentration calculated from the plot shown in panel a.

downconverted emission components. To best visualize broad-band light emission in the current chromophore mixture, the upconverted singlet fluorescence was, in essence, sacrificed by using high ground-state DMA concentrations to favor the production of the long wavelength excimer emission components. While the current approach provides a rather unique strategy for broad-band visible-light generation from a monochromatic light source, we anticipate that significant improvements could be realized using different classes of sensitizers in concert with other triplet acceptor/annihilators with a propensity for excimer formation.

Conclusion

Sensitized TTA photochemistry readily supports photon upconversion, yielding a significant population of singlet excited states poised for excimeric downconversion. Under appropriate conditions, the two processes can operate at similar efficiencies, producing well-balanced broad-band visible light potentially applicable for display and interior lighting technologies. Our present observations illustrate the viability of harnessing MLCT sensitized triplet annihilation processes for the production of broad-band white light using a low-energy monochromatic laser source at low power. As upconversion processes operate efficiently over a broad range of sensitizers and triplet acceptors/annihilators,[5,6] we anticipate that the current work can be extended to produce broad emission in other regions of interest across the electromagnetic spectrum.

Acknowledgment. This research was supported by the Air Force Office of Scientific Research (FA9550-05-1-0276), the NSF (CHE-0719050), the ACS-PRF (44138-AC3), and the BGSU Research Enhancement Initative. We are grateful to Dr. Aaron A. Rachford, who assisted in the acquisition of time-resolved emission spectra.

References and Notes

(1) (a) Yan, B.-P.; Cheung, C. C. C.; Kui, S. C. F.; Xiang, H.-F.; Roy, V. A. L.; Xu, S.-J.; Che, C.-M. *Adv. Mater.* **2007**, *19*, 3599−3603. (b) Yan, B.-P.; Cheung, C. C. C.; Kui, S. C. F.; Roy, V. A. L.; Xu, S.-J.; Che, C.-M. *Appl. Phys. Lett.* **2007**, *91*, 063508-1−063508-3. (c) Chan, S.-C.; Chan, M. C. W.; Wang, Y.; Che, C.-M. *Chem.—Eur. J.* **2001**, *7*, 4180−4190.

(2) (a) Adachi, C.; Baldo, M. A.; Forrest, S. R.; Thompson, M. E. *Appl. Phys. Lett.* **2000**, *77*, 904−906. (b) Adachi, C.; Baldo, M. A.; Forrest, S. R.; Lamansky, S.; Thompson, M. E.; Kwong, R. C. *Appl. Phys. Lett.* **2001**, *78*, 1622−1624. (c) D'Andrade, B. W.; Thompson, M. E.; Forrest, S. R. *Adv. Mater.* **2002**, *14*, 147−151. (d) Forrest, S. R.; Burrows, P. E.; Bulovic, V.; Kozlov, V.; Shen, Z.; Thompson, M. E. *Mater. Lett.* **1998**, *34*, 103−110. (e) Gu, G.; Garbuzov, D. Z.; Burrows, P. E.; Venkatesh, S.; Forrest, S. R.; Thompson, M. E. *Opt. Lett.* **1997**, *22*, 396−398.

(3) (a) Li, G.; Shinar, J.; Jabbour, G. E. *Phys. Rev. B: Condens. Matter Mater. Phys.* **2005**, *71*, 235211-1−235211-9. (b) Cheon, K. O.; Shinar, J. *Appl. Phys. Lett.* **2002**, *81*, 1738−1740. (c) Kim, C. H.; Shinar, J. *Appl. Phys. Lett.* **2002**, *80*, 2201−2203. (d) Lee, M. K.; Segal, M.; Soos, Z. G.; Shinar, J.; Baldo, M. A. *Phys. Rev. Lett.* **2006**, *96*, 089702-1.

(4) (a) D'Andrade, B. W.; Forrest, S. R. *Adv. Mater.* **2004**, *16*, 1585−1595. (b) Sun, Y.; Giebink, N. C.; Kanno, H.; Ma, B.; Thompson, M. E.; Forrest, S. R. *Nature (London, U.K.)* **2006**, *440*, 908−912. (c) Shinar, J. *Organic Light Emitting Devices*; Springer-Verlag: Berlin, 2004.

(5) (a) Koslov, D. V.; Castellano, F. N. *Chem. Commun. (Cambridge, U.K.)* **2004**, 2860−2861. (b) Islangulov, R. R.; Koslov, D. V.; Castellano, F. N. *Chem. Commun. (Cambridge, U.K.)* **2005**, 3776−3778. (c) Zhao, W.; Castellano, F. N. *J. Phys. Chem. A* **2006**, *110*, 11440−11445. (d) Islangulov, R. R.; Castellano, F. N. *Angew. Chem., Int. Ed.* **2006**, *45*, 5957−5959. (e) Islangulov, R. R.; Lott, J.; Weder, C.; Castellano, F. N. *J. Am. Chem. Soc.* **2007**, *129*, 12652−12653.

(6) (a) Keivanidis, P. E.; Baluschev, S.; Miteva, T.; Nelles, G.; Scherf, U.; Yasuda, A.; Wegner, G. *Adv. Mater.* **2003**, *15*, 2095−2098. (b) Baluschev, S.; Yu, F.; Miteva, T.; Ahl, S.; Yasuda, A.; Nelles, G.; Knoll, W.; Wegner, G. *Nano Lett.* **2005**, *5*, 2482−2484. (c) Laquai, F.; Wegner, G.; Im, C.; Büsing, A.; Heun, S. *J. Chem. Phys.* **2005**, *123*, 7, 074902-1−074902-6. (d) Baluschev, S.; Miteva, T.; Yakutkin, V.; Nelles, G.; Yasuda, A.; Wegner, G. *Phys. Rev. Lett.* **2006**, *97*, 143903−143905.

(7) (a) Barnes, R. L.; Birks, J. B. *Proc. R. Soc. London, Ser. A* **1966**, *291*, 570−582. (b) Parker, C. A.; Joyce, T. A. *J. Chem. Soc., Chem. Commun.* **1967**, *15*, 744−745.

(8) Damrauer, N. H.; Boussie, T. R.; Devenney, M.; McCusker, J. K. *J. Am. Chem. Soc.* **1997**, *119*, 8253−8268.

(9) Tyson, D. S.; Castellano, F. N. *J. Phys. Chem. A* **1999**, *103*, 10955−10960.

(10) Montalti, M.; Credi, A.; Prodi, L.; Gandolfi, M. T. *Handbook of Photochemistry*, 3rd ed.; CRC Press: Boca Raton, FL, 2005.

(11) Zalesskaya, G. A.; Pavlova, V. T.; Yakovlev, D. L.; Sambor, E. G.; Belyi, N. N. *Opt. Spectrosc.* **2002**, *93*, 920−928.

(12) Turro, N. J. *Modern Molecular Photochemistry*; The Benjamin-Cummings Publishing Co.: Menlo Park, CA, 1978.

(13) Lakowicz, J. R. *Principles of Fluorescence Spectroscopy*, 2nd ed.; Kluwer Academic/Plenum Publishers: New York, 1999.

(14) Wrighton, M.; Markham, J. *J. Phys. Chem.* **1973**, *77*, 3042−3044.